Single-Link Flexible Manipulator Control Accommodating Passivity Violations: Theory and Experiments

James Richard Forbes and Christopher John Damaren

***Abstract*—The robust control of a system which is nominally passive, but experiences a passivity violation is considered in this paper. Specifically, we utilize the hybrid passivity and finite gain stability theorem to robustly control a single-link flexible manipulator experiment. This system is nominally passive, but passivity is destroyed by, for example, sensor dynamics. The hybrid theorem is specifically applicable to such a scenario. We review and develop further the hybrid passivity and finite gain stability theorem in a linear time-invariant, single-input–single-output context. Calculation of the various passivity and finite gain parameters that classify a system as hybrid is discussed. In the interest of developing a hybrid controller that is optimal in some sense, we pose a numerical optimization problem which is constrained by the hybrid passivity and finite gain stability theorem. The numerical optimization objective function seeks to have a hybrid controller mimic a nominal $\mathcal{H}_2$ controller. Experimental results successfully demonstrate tip-based feedback control of a single-link flexible manipulator.**

***Index Terms*—Controller optimization, passivity-based control, passivity violations, single-link manipulator, tip-control, vibration control.**

I. Introduction

PASSIVE systems and passivity-based control schemes have been actively researched for several decades [1], [2]. Passivity-based control relies on the passivity theorem which states that a very strictly passive controller will stabilize a passive plant when connected in a negative feedback loop [3]. Passivity-based control schemes are attractive owing to the robustness properties of the closed-loop.

The control of flexible systems, especially those of aerospace origin, is an interesting control challenge that has been previously investigated in the literature [4]–[7]. Passivity-based control is often used to control flexible, lightly damped systems. As a result of very little natural damping, the gain of these flexible systems is nominally quite high, and stabilization via other theorems is overly restrictive. For example, the small gain theorem states that the negative feedback interconnection of two systems will be stable provided the product of the plant gain and controller gain is less than one [3]. Given that flexible systems have high gain, the controller gain must be very small if the small gain theorem is to ensure stability of the closed-loop system. This in turn leads to poor closed-loop performance. Passivity-based control, however, places no gain restriction on the plant, and less restrictive gain limitations on the control. This allows implementation of much more aggressive control laws. For example, in [8] strictly positive real (SPR) rate controllers (which are very strictly passive when modified slightly) are used to control large space structures. In [9], the control of large space structures using linear quadratic Gaussian (LQG) controllers which maintain SPRness was considered. Recently in [10] the control of n-link flexible manipulators using optimal gain-scheduled SPR controllers was considered.

In the context of n-link flexible robot manipulators, a passive map between the joint torques and the angular joint rates exists owing to collocation of the actuators and sensors. The importance of actuator and sensor collocation whilst controlling flexible systems was first pointed out in [11]. When excellent end-effector position and rate control is required, it is not sufficient to suppress vibration of the links at the joint level, but rather the manipulator end-effector position and rate must explicitly be controlled. Unfortunately, the map between the manipulator joint torques and tip rate is not passive, and the passivity theorem can not be employed to robustly stabilize the system. However, while carrying large payloads a passive input-output map between a modified joint torque and a modified tip rate, known as the μ-tip rate, does exist as shown in [12]. In [12], passivity-based control of n-link flexible manipulators using the μ-tip rate is considered, and in [13] the effectiveness of using the μ-tip rate is demonstrated experimentally using a three-link manipulator test bed. In [14] an upper bound for the parameter μ is found based on the collocated and noncollocated mass ratios of the system when the payload is large, but not quite massive. The μ-tip framework is applicable to nonlinear, multi-input-multi-output (MIMO) systems, as well as linear single-input-single-output (SISO) systems. The work of [12], that is defining and controlling a modified input-output map that is passive, was originally inspired by [15] and [16] where the map between the joint torque and the reflected tip rate of a single-link flexible manipulator was considered. Similarly, in [17] the control of a point along a flexible manipulator, inboard of the tip, was investigated, which is similar to the ideas explored in [12], [15], and [16].

Often while employing passivity-based control the affect of unmodeled sensors and actuators is overlooked. Usually it is assumed that the sensors and actuators (e.g., encoders, tachometers, potentiometers, electrical motors, peizoelectric actuators, etc.) have dynamics which possess infinite bandwidth and unity

Manuscript received August 09, 2010; revised November 10, 2010; accepted February 13, 2011. Manuscript received in final form February 26, 2011. Date of publication April 05, 2011; date of current version April 11, 2012. Recommended by Associate Editor A. G. Alleyne.

J. R. Forbes and C. J. Damaren are with the University of Toronto Institute for Aerospace Studies, Toronto, ON M3H 5T6, Canada (e-mail: forbes@utias.utoronto.ca; damaren@utias.utoronto.ca).

Color versions of one or more of the figures in this paper are available online at http://ieeexplore.ieee.org.

Digital Object Identifier 10.1109/TCST.2011.2122307

gain. In practice, such an assumption is false, and these unmodeled dynamics destroy the nominally passive nature of the system under control; they induce a *passivity violation*.

In [18] the hybrid passivity and finite gain stability theorem is presented in a general nonlinear MIMO context. Plants which are nominally passive, but have somehow had their passivity destroyed by, for example, sensor and actuator dynamics is the motivation behind this theorem. A hybrid system is a continuous system which possesses a passive input-output map and a finite gain input-output map when the passive input-output map no longer exists (i.e., passivity has been violated). Hybrid systems are similar to "mixed" systems [19], [20] and finite frequency positive real systems [21]. The hybrid passivity and finite gain stability theorem utilizes both the passivity theorem and the small gain theorem in tandem; stability is guaranteed via the passivity theorem when a passive input-output map exists, but when a passivity violation occurs above a critical frequency, gain bounds on the plant and control ensure the closed-loop system is stable. This theorem formalizes what has, at least practically, always been known: passivity violations (i.e., phase violations in the linear time-invariant sense) that occur at high frequency are not destabilizing provided the gain of the plant, controller, sensors, and actuators has naturally subsided (i.e., the gain of each rolls off). The word "hybrid" is used to highlight the fact that within the hybrid passivity/finite gain framework closed-loop stability is not guaranteed by the passivity theorem alone, and not by the small gain theorem alone, but rather by both passive and finite gain means in a "hybrid", "tandem", "mixed", or "blended" fashion. Our use of the word hybrid does not include, describe, nor refer to systems which employ some sort of discrete switching.

The purpose of this paper is to implement, and validate experimentally, the hybrid passivity/finite gain stability theorem in terms of SISO control of a single-link flexible manipulator. This linear time-invariant (LTI) plant is nominally passive, but experiences a passivity violation when, for example, sensor dynamics are considered. We review hybrid systems theory and future develop it in a LTI, SISO context. We show how to calculate the passivity and finite gain parameters which are used to assess closed-loop stability of hybrid systems. We also present a controller optimization formulation: the frequency response of a transfer function is numerically optimized to mimic a traditional $\mathcal{H}_2$ controller while simultaneously being constrained to satisfy the hybrid passivity/finite gain stability theorem. In turn, when the transfer function is employed as a controller, closed-loop stability is guaranteed. Last, an optimized hybrid controller is used to control a single-link flexible manipulator experimental apparatus, demonstrating the utility and success of the hybrid theory and optimization formulation.

II. Single-Link Flexible Manipulator

A. Input-Output Model

In this study we will control the tip position and rate of a planar single-link flexible manipulator carrying a large payload described by

$$\mathbf{M}\ddot{\mathbf{q}} + \mathbf{D}\dot{\mathbf{q}} + \mathbf{K}\mathbf{q} = \mathbf{b}\tau \tag{1}$$

where $\mathbf{M} > 0$, $\mathbf{D} \geq 0$, and $\mathbf{K} \geq 0$ are the mass, damping, and stiffness matrices, $\mathbf{b} = [1\ \mathbf{0}]^\mathsf{T}$, τ is the joint torque, $\mathbf{q} = [\theta\ \mathbf{q}_e^\mathsf{T}]^\mathsf{T}$, θ is the joint angle of the hub, and $\mathbf{q}_e$ are the elastic coordinates associated with the flexible link discretization. A nonplanar system can just as easily be considered; gravity may be considered a known disturbance and compensated by a feedforward control scheme.

The output we are interested in controlling is the μ-tip rate [12], [13]

$$y := \dot{\rho}_\mu = J_\theta \dot{\theta} + \mu \mathbf{J}_e \dot{\mathbf{q}}_e \tag{2}$$

where J_θ is the rigid Jacobian, $\mathbf{J}_e$ is the elastic Jacobian, and μ is a fixed scalar parameter that will help us define a passive input-output map. When $\mu = 1$ the output is the true-tip rate, $\dot{\rho} = \dot{\rho}_{\mu=1}$, when $\mu = 0$ the output is the rigid-tip rate, and when $\mu = -1$ the output is the reflected-tip rate as discussed in [15] and [16]. Various authors have considered true-tip position and rate control; for example, one of the earliest works is [22]. The noncollocated mapping between the joint torque and the true-tip rate is nonminimum phase, and hence not passive. However, if $0 \leq \mu < 1$ and the manipulator is carrying a large payload, a passive input-output map can be defined.

Scaling $\mathbf{J}_e$ by μ when $0 \leq \mu < 1$ can be thought of as artificially retarding the natural flexibility of the link. From (2) we can equivalently write $\dot{\rho}_\mu$ as

$$\begin{aligned}\dot{\rho}_\mu &= J_\theta \dot{\theta} + \mu \mathbf{J}_e \dot{\mathbf{q}}_e + \mu J_\theta \dot{\theta} - \mu J_\theta \dot{\theta} \\ &= (1-\mu) J_\theta \dot{\theta} + \mu \underbrace{(J_\theta \dot{\theta} + \mathbf{J}_e \dot{\mathbf{q}}_e)}_{\dot{\rho}} \\ &= (1-\mu) J_\theta \dot{\theta} + \mu \dot{\rho}.\end{aligned} \tag{3}$$

The above provides an expression for the μ-tip position

$$\rho_\mu = (1-\mu) J_\theta \theta + \mu \rho. \tag{4}$$

By defining $u = J_\theta^{-1}\tau$, which will be referred to as the modified joint torque, we can capture the modified input-output dynamics in terms of a transfer function

$$\begin{aligned} y(s) &= g(s)u(s) \\ g(s) &= \frac{M_{\theta\theta}^{-1} J_\theta^2}{s} + \sum_{\alpha=1}^{N_e} \frac{s}{s^2 + 2\zeta_\alpha \omega_\alpha s + \omega_\alpha^2} c_\alpha b_\alpha \\ c_\alpha &= J_\theta \theta_\alpha + \mu \mathbf{J}_e \mathbf{q}_{e\alpha} \\ b_\alpha &= \theta_\alpha J_\theta, \quad \alpha = 1, \ldots, N_e \end{aligned} \tag{5}$$

where $y(s) = s\rho_\mu(s)$, $u(s) = J_\theta^{-1}\tau(s)$, $M_{\theta\theta}$ is the rigid portion of the mass matrix, and ζ_α and ω_α are the damping ratios and natural frequencies associated with the N_e modes of the flexible link. The eigenvectors corresponding to the undamped, unforced form of (1) are $\mathbf{q}_\alpha = [\theta_\alpha\ \mathbf{q}_{e\alpha}^\mathsf{T}]^\mathsf{T}$. The transfer function $g(s)$ follows from modal decomposition of (1) and (2), followed by use of the Laplace transform. While carrying a large payload, the above transfer function is passive, that is positive real, provided $0 \leq \mu < 1$. Recall a positive real transfer function has phase bounded by $\pm 90^\circ$, i.e., $-\pi/2 \leq \arg g(j\omega) \leq \pi/2$ $\forall \omega \in \mathbb{R}$. Because $u(s) \to y(s)$ is a passive input-output map,

robust closed-loop stability is guaranteed via the passivity theorem when a very strictly passive controller is employed. For example

$$-u(s) = \left[\frac{K_p}{s} + g_{\mathrm{VSP}}(s)\right] y(s)$$

where K_p is the proportional control gain and $g_{\mathrm{VSP}}(s)$ is a very strictly passive transfer function would realize robust stabilization with respect to uncertain manipulator mass and stiffness. Unfortunately, the modified output $y(s)$ is generally not directly available, as discussed in the next section.

B. Violation of Passivity

At any given time θ and ρ are measured, and ρ_μ can be calculated using (4). Using ρ_μ, proportional control of the form $K_p\rho_\mu(s)$ can be applied to the system without issue because proportional control does not alter the passivity of the system. Let $\rho_\mu(s) = g_p(s)u(s)$ be the plant with proportional control included. In order to implement rate control $\dot\rho_\mu$ is needed. By filtering ρ_μ with a derivative filter $f(s)$, $\dot\rho_\mu$ can be approximated as $y_1(s) = f(s)\rho_\mu(s)$. If $f(s) = s$, that is perfect differentiation were possible, $y_1(s) \equiv \dot\rho_\mu(s)$ and use of the traditional passivity theorem would be appropriate. Unfortunately, a real derivative filter possesses dynamics and has a finite bandwidth; a realistic derivative filter is

$$f(s) = s\left(\frac{\omega_f^2}{s^2 + 2\zeta_f\omega_f s + \omega_f^2}\right) \tag{6}$$

and as a result the true plant output (which is the controller input) is really $y_1(s) = g_1(s)u(s)$, where $g_1(s) = f(s)g_p(s)$. Although the nominal plant $g(s)$ is passive, $g_1(s)$ is not passive owing to the presence of the filter $f(s)$. Fortunately, however, $g_1(s)$ is still passive within a bandwidth; in a low frequency region the passive characteristics of $g(s)$ are maintained because $f(s)$ essentially has no phase delay. As such, we would expect $g_1(s)$ to be phase bounded by $\pm 90^\circ$ at low frequency. At high frequency, however, $f(s)$ induces phase delay, thus destroying the positive realness of the plant; $g_1(s)$ is expected to have phase that exceeds $\pm 90^\circ$, that is to say passivity is violated at high frequency. However, in this high frequency region the plant will have finite gain due to the roll off of the both $g_p(s)$ and $f(s)$. The plant $g_1(s)$ can be segmented into two parts: a low frequency passive (i.e., positive real) part, and a high frequency finite gain part. The hybrid passivity/finite gain framework is ideal for such systems.

III. Linear Hybrid Passivity/Finite Gain Stability Theory

Here we will review the definition of a hybrid system, and the hybrid passivity/finite gain stability theorem in the context of LTI, SISO systems. This theory is fully developed in a general context (i.e., MIMO and nonlinear) in [18].

Recall that a time dependent function $y \in L_2$ if $\int_0^\infty y^2(t)\,dt = (1)/(2\pi)\int_{-\infty}^\infty y(-j\omega)y(j\omega)\,d\omega < \infty$ and $y \in L_{2e}$ if $\int_0^T y^2(t)\,dt = (1)/(2\pi)\int_{-\infty}^\infty y_T(-j\omega)y_T(j\omega)\,d\omega < \infty$, $0 \le T < \infty$, where $y_T(t) = y(t)$, $0 \le t \le T$ and $y_T(t) = 0$, $t > T$. We abuse notation and $y(j\omega)$ denotes the Fourier transform of y.

A. SISO, LTI Hybrid Systems

Consider a LTI, SISO system mapping inputs $e \in L_{2e}$ to outputs $y \in L_{2e}$ through the operator $G : L_{2e} \to L_{2e}$, that is $y(t) = (Ge)(t)$. Via Laplace transforms the system mapping may be expressed as $y(s) = g(s)e(s)$, where $g(s) \in \mathbb{C}$ is the system transfer function. The system is considered a hybrid passive/finite gain system if

$$\begin{aligned}\frac{1}{2\pi}\int_{-\infty}^{\infty} & y_T(-j\omega)Q(\omega)y_T(j\omega)\,d\omega \\ &+ \frac{1}{\pi}\mathrm{Re}\int_{-\infty}^{\infty} y_T(-j\omega)S(\omega)e_T(j\omega)\,d\omega \\ &+ \frac{1}{2\pi}\int_{-\infty}^{\infty} e_T(-j\omega)R(\omega)e_T(j\omega)\,d\omega \ge 0\end{aligned} \tag{7}$$

where

$$\begin{aligned}Q(\omega) &= -[\epsilon\alpha(\omega) + \gamma^{-1}(1-\alpha(\omega))] \\ S(\omega) &= \frac{1}{2}\alpha(\omega) \\ R(\omega) &= [\gamma(1-\alpha(\omega)) - \delta\alpha(\omega)].\end{aligned} \tag{8}$$

The constant parameters δ and ϵ depend on the passive nature of the system, and γ depends on the finite gain nature of the system. Notice the units of Q and R are consistent; ϵ and γ^{-1} have units of one over gain, while δ and γ have units of gain. The frequency variable $\alpha : \mathbb{R} \to \{0,1\}$ is a theoretical abstraction used to distinguish between passive system characteristics and nonpassive but still finite gain system characteristics. When the system in question possesses a passive input-output map, $\alpha(\omega) = 1$. When the system fails to possess a passive input-output map, that is the system has experienced a passivity violation, but the map has finite gain, $\alpha(\omega) = 0$. The divide occurs at a critical frequency, ω_c, which is used to define α:

$$\begin{aligned}\alpha(\omega) &= \begin{cases} 1, & -\omega_c < \omega < \omega_c \quad \text{(passive region)} \\ 0, & |\omega| \ge \omega_c \quad \text{(finite gain region)}\end{cases} \\ &= A(-j\omega)A(j\omega) \\ &= |A(j\omega)|^2.\end{aligned}$$

The transfer function $A(s)$ is causal and can be expressed by the operator $\mathcal{A} : L_2 \to L_2$. We can intuitively think of α as an ideal low pass filter, filtering the signals into two parts: a passive part and a finite gain part.

When the system maintains passive properties $\alpha(\omega) = 1$ and (7) reduces to

$$\begin{aligned}\frac{1}{2\pi}\mathrm{Re}\int_{-\omega_c}^{\omega_c} y_T(-j\omega)e_T(j\omega)\,d\omega \ge \frac{\delta}{2\pi}\int_{-\omega_c}^{\omega_c}|e_T(j\omega)|^2\,d\omega \\ + \frac{\epsilon}{2\pi}\int_{-\omega_c}^{\omega_c}|y_T(j\omega)|^2\,d\omega.\end{aligned}$$

Within this frequency band we say that the hybrid system has characteristics which are as follows:

1) passive when $\delta = \epsilon = 0$;
2) very strictly passive, or input strictly passive with finite gain when $\delta > 0$ and $\epsilon > 0$;
3) input strictly passive when $\delta > 0$ and $\epsilon = 0$;
4) output strictly passive when $\delta = 0$ and $\epsilon > 0$.

Upon violation of passivity, $\alpha(\omega) = 0$, and (7) gives

$$\frac{1}{\pi\gamma}\int_{\omega_c}^{\infty}|y_T(j\omega)|^2\,d\omega \le \frac{\gamma}{\pi}\int_{\omega_c}^{\infty}|e_T(j\omega)|^2\,d\omega.$$

Within this frequency band we say the system has finite gain.

Notice that if a passivity violation does not occur at all, then $\omega_c = \infty$ and from (7) and (8) the traditional definition of a input strictly, output strictly, very strictly, or simply passive system is recovered. Similarly, if $\omega_c = 0$, that is the system possess a map which is never passive but does have finite gain, the traditional definition of a finite gain system is recovered.

B. Defining Hybrid Parameters for SISO, LTI Hybrid Systems

We will start by defining the input strictly passive parameter δ

$$\begin{aligned}
&\frac{1}{2\pi}\mathrm{Re}\int_{-\omega_c}^{\omega_c} e_T(-j\omega)y_T(j\omega)\,d\omega \\
&\quad = \frac{1}{2\pi}\mathrm{Re}\int_{-\omega_c}^{\omega_c} e_T(-j\omega)[g(j\omega)e_T(j\omega)]\,d\omega \\
&\quad \geq \underbrace{\inf_{-\omega_c<\omega<\omega_c}\mathrm{Re}\{g(j\omega)\}}_{\delta}\ \frac{1}{2\pi}\mathrm{Re}\int_{-\omega_c}^{\omega_c}|e_T(j\omega)|^2\,d\omega \\
&\quad = \frac{\delta}{2\pi}\int_{-\omega_c}^{\omega_c}|e_T(j\omega)|^2\,d\omega \qquad (9)
\end{aligned}$$

where $\mathrm{Re}\{\cdot\}$ represents the real part. Therefore, $\delta = \inf_{-\omega_c<\omega<\omega_c}\mathrm{Re}\{g(j\omega)\}$.

Next we will consider the output strictly passive parameter ϵ in the context of a finite gain, input strictly passive hybrid system, i.e., a very strictly passive hybrid system. An input strictly passive hybrid system that possesses finite gain satisfies (9) in addition to

$$\frac{1}{2\pi\kappa^2}\int_{-\omega_c}^{\omega_c}|y_T(j\omega)|^2\,d\omega \leq \frac{1}{2\pi}\int_{-\omega_c}^{\omega_c}|e_T(j\omega)|^2\,d\omega \qquad (10)$$

where κ, the gain of the system over $-\omega_c < \omega < \omega_c$, can be calculated in the following way:

$$\begin{aligned}
&\frac{1}{2\pi}\int_{-\omega_c}^{\omega_c}|y_T(j\omega)|^2\,d\omega \\
&\quad = \frac{1}{2\pi}\int_{-\omega_c}^{\omega_c}|g(j\omega)e_T(j\omega)|^2\,d\omega \\
&\quad \leq \underbrace{\sup_{-\omega_c<\omega<\omega_c}|g(j\omega)|^2}_{\kappa^2}\ \frac{1}{2\pi}\int_{-\omega_c}^{\omega_c}|e_T(j\omega)|^2\,d\omega \\
&\quad = \frac{\kappa^2}{2\pi}\int_{-\omega_c}^{\omega_c}|e_T(j\omega)|^2\,d\omega.
\end{aligned}$$

Therefore, $\kappa = \sup_{-\omega_c<\omega<\omega_c}|g(j\omega)|$ and is referred to as the passive system gain. To show that an input strictly passive, finite gain hybrid system is in fact very strictly passive when passivity holds, we will start with (9), let $\bar{\delta} = \delta/2$, and then manipulate using (10) [23]

$$\begin{aligned}
&\frac{1}{2\pi}\mathrm{Re}\int_{-\omega_c}^{\omega_c} e_T(-j\omega)y_T(j\omega)\,d\omega \\
&\quad \geq \frac{\bar{\delta}}{2\pi}\int_{-\omega_c}^{\omega_c}|e_T(j\omega)|^2\,d\omega + \frac{\bar{\delta}}{2\pi}\int_{-\omega_c}^{\omega_c}|e_T(j\omega)|^2\,d\omega \\
&\quad \geq \frac{\bar{\delta}}{2\pi}\int_{-\omega_c}^{\omega_c}|e_T(j\omega)|^2\,d\omega + \underbrace{\frac{\bar{\delta}}{\kappa^2}}_{\bar{\epsilon}}\frac{1}{2\pi}\int_{-\omega_c}^{\omega_c}|y_T(j\omega)|^2\,d\omega.
\end{aligned}$$

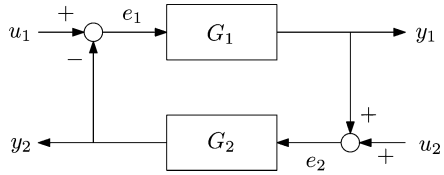

Fig. 1. General negative feedback interconnection of systems G_1 and G_2.

Therefore, a finite gain, input strictly hybrid passive system is clearly a very strictly passive hybrid system. Henceforth, stating a very strictly passive hybrid system has $\delta > 0$ and $\kappa < \infty$ implies $\delta > 0$ and $\epsilon > 0$.

The gain of the system when passivity has been violated can be calculated via

$$\frac{1}{\pi}\int_{\omega_c}^{\infty}|y_T(j\omega)|^2\,d\omega \leq \underbrace{\sup_{\omega\geq\omega_c}|g(j\omega)|^2}_{\gamma^2}\frac{1}{\pi}\int_{\omega_c}^{\infty}|e_T(j\omega)|^2\,d\omega. \qquad (11)$$

Therefore, $\gamma = \sup_{\omega\geq\omega_c}|g(j\omega)|$.

It should be clear that the parameters δ, ϵ, and γ associated with a hybrid passive/finite gain system are not equivalent to the traditional definitions associated with completely passive systems or completely finite gain systems. Here we have defined δ, ϵ, and γ over specific frequency bands. In the traditional definitions these parameters are defined over all frequencies.

C. Stability of Interconnected Hybrid Passive/Finite Gain Systems

Consider the negative feedback interconnection of two hybrid systems presented in Fig. 1. The passivity and finite gain parameters for each system G_1 and G_2 are defined as δ_1, ϵ_1, and γ_1 and δ_2, ϵ_2, and γ_2, respectively.

Theorem 3.1—Hybrid Passivity and Finite Gain Stability Theorem: Given that $G_1 : L_{2e} \to L_{2e}$ and $G_2 : L_{2e} \to L_{2e}$, the negative feedback interconnection presented in Fig. 1 is L_2-stable if the variables δ_1, ϵ_1, γ_1, δ_2, ϵ_2, and γ_2 satisfy $\epsilon_1 + \delta_2 > 0$, $\epsilon_2 + \delta_1 > 0$, and $\gamma_1\gamma_2 < 1$.

Proof: See [18]. □

The hybrid passivity and finite gain stability theorem as stated above is a fusion of the passivity theorem and the small gain theorem. It allows the control gain to be large within the corresponding passive frequency band of the plant being controlled. When the plant has its passivity violated but maintains finite gain the control is then required to satisfy a gain constraint, that is $\gamma_1\gamma_2 < 1$, but only outside of the passive frequency band. The hybrid passivity and finite gain stability theorem allows high gain compensation to be reintroduced (in a frequency band) where the traditional small gain theorem would be overly conservative and the traditional passivity theorem alone would not guarantee stability at all.

In this paper, the plant to be controlled is a single-link flexible manipulator. As discussed in Section II-B the nominal plant is passive, but in reality passivity is violated as a result of rate signal approximation via the filter $f(s)$. The system has become hybrid possessing passive dynamics at low frequency, and finite

gain dynamics above a critical frequency. With the hybrid systems theory at our disposal, provided we design a controller to satisfy the hybrid stability criteria discussed above, closed-loop stability can be guaranteed. The optimal design of such a controller is the topic of Section IV.

IV. Controller Design and Synthesis

The hybrid passivity and finite gain stability theorem provides sufficient conditions for closed-loop stability. The theorem does not address how to design an optimal controller for a specific plant. The traditional $\mathcal{H}_2$ formulation yields an optimal controller given certain weighting matrices on the states, control, disturbances, and noise. In theory, a $\mathcal{H}_2$ controller should work exceptionally well in any situation, but in practice unmodeled plant dynamics and excessive noise often lead to poor closed-loop system characteristics, and in some cases an unstable closed loop.

Knowing that a $\mathcal{H}_2$ controller should yield a closed-loop with an optimal system response, we seek a controller that mimics the $\mathcal{H}_2$ solution as closely as possible, but simultaneously satisfies the hybrid passivity/finite gain stability theorem in order to provide robustness. To find such a controller, we will pose a numerical optimization problem. Although the plant we wish to eventually control is SISO, for generality we will pose our numerical optimization problem in a MIMO context.

To properly pose our numerical optimization problem, let us review the traditional $\mathcal{H}_2$ formulation [24]. The nominal system (i.e., one which ignores sensors, actuators, etc., which induce passivity violations) to be controlled is

$$\begin{aligned}\dot{\mathbf{x}} &= \mathbf{A}\mathbf{x}+\mathbf{B}_1\mathbf{w}+\mathbf{B}_2\mathbf{u}\\ \mathbf{z} &= \mathbf{C}_1\mathbf{x}+\mathbf{D}_{12}\mathbf{u}\\ \mathbf{y} &= \mathbf{C}_2\mathbf{x}+\mathbf{D}_{21}\mathbf{w}\end{aligned}$$

where $\mathbf{x}\in\mathbb{R}^n$ is the system state, $\mathbf{u}\in\mathbb{R}^{n_u}$ is the control input, $\mathbf{y}\in\mathbb{R}^{n_y}$ is the measurement, $\mathbf{z}\in\mathbb{R}^{n_z}$ is the regulated output, the disturbances/noise are $\mathbf{w}=[\mathbf{d}^\top\ \mathbf{v}^\top]^\top\in\mathbb{R}^{n_w}$, and all matrices are dimensioned appropriately. The following is assumed:

1) $(\mathbf{A},\mathbf{B}_1)$ is controllable and $(\mathbf{C}_1,\mathbf{A})$ is observable;
2) $(\mathbf{A},\mathbf{B}_2)$ is controllable and $(\mathbf{C}_2,\mathbf{A})$ is observable;
3) $\mathbf{D}_{12}^\top\mathbf{C}_1=\mathbf{0}$ and $\mathbf{D}_{12}^\top\mathbf{D}_{12}>0$;
4) $\mathbf{D}_{21}\mathbf{B}_1^\top=\mathbf{0}$ and $\mathbf{D}_{21}\mathbf{D}_{21}^\top>0$.

The $\mathcal{H}_2$ optimal controller takes the following form:

$$\left.\begin{aligned}\dot{\mathbf{x}}_c &= \overbrace{(\mathbf{A}-\mathbf{B}_2\mathbf{K}_c-\mathbf{K}_e\mathbf{C}_2)}^{\mathbf{A}_c^\star}\mathbf{x}_c+\overbrace{\mathbf{K}_e}^{\mathbf{B}_c^\star}\mathbf{y}\\ -\mathbf{u} &= \underbrace{\mathbf{K}_c}_{\mathbf{C}_c^\star}\mathbf{x}_c\end{aligned}\right\}$$
$$\Leftrightarrow -\mathbf{u}(s)=\mathbf{G}^\star(s)\mathbf{y}(s)=\mathbf{C}_c^\star(s\mathbf{1}-\mathbf{A}_c^\star)^{-1}\mathbf{B}_c^\star\mathbf{y}(s) \quad (12)$$

where $\mathbf{K}_c$ is the optimal feedback gain matrix and $\mathbf{K}_e$ is the optimal observer gain matrix.

Now let us move on to formulating our numerical optimization problem. Consider a plant that is nominally passive, although passivity will be destroyed via sensors, actuators, etc., rendering the true plant hybrid. Estimated values of the critical frequency, ω_c, and the high frequency gain, γ_1, associated with the hybrid plant are assumed available (via approximate modeling, for example), for the true passivity violation is never fully known. To be conservative we assume $\delta_1=0$ and $\kappa_1\approx\infty$. Assuming $\delta_1=0$ is reasonable because the nominal plant to be controlled is passive/positive real. Assuming $\kappa_1\approx\infty$ is reasonable because, again, the nominal plant is passive, but also the system to be controlled most likely has finite gain, but it is difficult to characterize (such as in the context of flexible manipulator control). Therefore, a conservative assumption is $\kappa_1\approx\infty$.

Given our assumptions and an estimated passivity violation, for the closed-loop to be stable the controller $\mathbf{G}_2(s)$ must satisfy $\delta_2>0$, $\kappa_2<\infty$, and $\gamma_1\gamma_2<1$. A $\mathcal{H}_2$ design provides the controller $\mathbf{G}_2^\star(s)$. This controller will not necessarily satisfy the hybrid requirements (it may by chance, however), but will perform well in simulation; it is optimal but not generally robust.

Let $\mathbf{W}(s)$ be a filter, $\mathbf{G}_{2,w}(s)=\mathbf{G}_2(s)\mathbf{W}(s)$, and $\mathbf{G}_{2,w}^\star(s)=\mathbf{G}_2^\star(s)\mathbf{W}(s)$, where

$$\begin{aligned}\mathbf{W}(s) &= \left[\begin{array}{c|c}\mathbf{A}_w & \mathbf{B}_w\\ \hline \mathbf{C}_w & \mathbf{D}_w\end{array}\right]\\ \mathbf{G}_2(s) &= \left[\begin{array}{c|c}\mathbf{A}^\star & \mathbf{B}^\star\\ \hline \mathbf{C} & \mathbf{0}\end{array}\right]\\ \mathbf{G}_2^\star(s) &= \left[\begin{array}{c|c}\mathbf{A}^\star & \mathbf{B}^\star\\ \hline \mathbf{C}^\star & \mathbf{0}\end{array}\right]\\ \mathbf{G}_{2,w}(s) &= \left[\begin{array}{c|c}\bar{\mathbf{A}} & \bar{\mathbf{B}}\\ \hline [\mathbf{C}\ \ \mathbf{0}] & \mathbf{0}\end{array}\right]\\ \mathbf{G}_{2,w}^\star(s) &= \left[\begin{array}{c|c}\bar{\mathbf{A}} & \bar{\mathbf{B}}\\ \hline [\mathbf{C}^\star\ \ \mathbf{0}] & \mathbf{0}\end{array}\right].\end{aligned} \quad (13)$$

The matrices $\bar{\mathbf{A}}$ and $\bar{\mathbf{B}}$ depend on both the controller and filter state-space matrices

$$\bar{\mathbf{A}}=\begin{bmatrix}\mathbf{A}^\star & \mathbf{B}^\star\mathbf{C}_w\\ \mathbf{0} & \mathbf{A}_w\end{bmatrix},\quad \bar{\mathbf{B}}=\begin{bmatrix}\mathbf{B}^\star\mathbf{D}_w\\ \mathbf{B}_w\end{bmatrix}.$$

Notice that the only difference between the $\mathcal{H}_2$ controller, $\mathbf{G}_2^\star(s)$, and the hybrid controller, $\mathbf{G}_2(s)$, to be optimally designed is the matrix $\mathbf{C}$. Let

$$\begin{aligned}\mathbf{H}(s) &= \left[\begin{array}{c|c}\bar{\mathbf{A}} & \bar{\mathbf{B}}\\ \hline \bar{\mathbf{C}} & \mathbf{0}\end{array}\right]\\ &= \mathbf{G}_{2,w}^\star(s)-\mathbf{G}_{2,w}(s)\\ &= [\mathbf{G}_2^\star(s)-\mathbf{G}_2(s)]\mathbf{W}(s)\end{aligned}$$

which represents the filtered difference between the two controllers.

Consider the following objective function [25]:

$$\mathcal{J}(\mathbf{C})=\frac{1}{2\pi}\int_{-\infty}^{\infty}\operatorname{tr}\mathbf{H}(j\omega)\mathbf{H}^\top(-j\omega)d\omega.$$

Our objective function minimizes the filtered difference between $\mathbf{G}_{2,w}^\star(s)$ and $\mathbf{G}_{2,w}(s)$ over all frequencies. The filter adds flexibility into the design of $\mathbf{G}_2(s)$. Letting $\mathbf{W}(s)$ be lowpass allows $\mathbf{G}_2^\star(s)$ and $\mathbf{G}_2(s)$ to differ at high frequency, while letting $\mathbf{W}(s)=\mathbf{1}$ ensures $\mathbf{G}_2(s)$ is as close to $\mathbf{G}_2^\star(s)$ as possible over all frequencies. The above objective function can be written as

$$\mathcal{J}(\mathbf{C})=\operatorname{tr}(\mathbf{C}-\mathbf{C}^\star)^\top\mathbf{L}(\mathbf{C}-\mathbf{C}^\star)$$

where $\mathbf{L}$ is the upper $n \times n$ part of the matrix $\bar{\mathbf{L}}$ which is the solution of the Lyapunov equation $\bar{\mathbf{L}}\bar{\mathbf{A}} + \bar{\mathbf{A}}^{\mathsf{T}}\bar{\mathbf{L}} = -\bar{\mathbf{B}}\bar{\mathbf{B}}^{\mathsf{T}}$. In a SISO context $\mathcal{J}(\mathbf{C}) = (\mathbf{C}-\mathbf{C}^{\star})^{\mathsf{T}}\mathbf{L}(\mathbf{C}-\mathbf{C}^{\star})$ because $\mathbf{C}, \mathbf{C}^{\star} \in \mathbb{R}^{1\times n}$.

We are now poised to state our numerical optimization problem.

Design Variables: The elements of $\mathbf{C}$.

Constraints: $\mathbf{G}_2(s)$ must satisfy $\delta_2 > 0$, $\kappa_2 < \infty$, and $\gamma_1\gamma_2 < 1$.

Objective Function: Minimize $\mathcal{J}(\mathbf{C}) = \mathrm{tr}(\mathbf{C} - \mathbf{C}^{\star})^{\mathsf{T}}\mathbf{L}(\mathbf{C} - \mathbf{C}^{\star})$.

It is worth noting that we have chosen the above parameterization because it is simple; the SISO form of the objective function $\mathcal{J}(\mathbf{C}) = (\mathbf{C}-\mathbf{C}^{\star})^{\mathsf{T}}\mathbf{L}(\mathbf{C}-\mathbf{C}^{\star})$ has a quadratic form ideal for numerical optimization.

The numerical algorithm employed to solve our optimization problem will be a sequential quadratic programming (SQP) algorithm where constraints are enforced via Lagrange multipliers and derivative information is acquired via finite differencing [26]. A SQP that employs finite differencing is used because it is simple to setup the optimization problem; only the objective function and the constraints must be provided to the optimizer. In particular, the optimization software we will use to solve our problem is `fmincon` within MATLAB's optimization toolbox.

Before continuing, some comments on our controller design and synthesis method are in order. The way we go about designing a hybrid controller involves two approximations. First, it would be best if we could somehow synthesize a controller by directly minimizing the closed-loop $\mathcal{H}_2$ norm subject to a set of constraints which ensure the controller is hybrid. Unfortunately, doing so is rather intractable; instead we are minimizing the difference (in an $\mathcal{H}_2$ sense) between our hybrid controller and an unconstrained $\mathcal{H}_2$ controller. This is our first approximation which is done so that our problem (that is, synthesizing a hybrid controller that is close to optimal) is tractable. Second, we parameterize our hybrid controller in terms of feedback gain matrix $\mathbf{C}$; the dynamics matrix and input matrix of $\mathbf{G}_2(s)$ are taken from the $\mathcal{H}_2$ controller $\mathbf{G}_2^{\star}(s)$ [i.e., both $\mathbf{G}_2(s)$ and $\mathbf{G}_2^{\star}(s)$ use $\mathbf{A}^{\star}$ and $\mathbf{B}^{\star}$; see (13)]. This is our second approximation which leads to a tractable optimization problem easily solved by a numerical solver such as a SQP algorithm. To summarize, our controller design and synthesis procedure employs two approximations which leads to an optimization problem that can be easily solved.

V. Experimental Implementation and Results

A. Experimental Apparatus

The theoretical developments discussed in the previous sections will be tested on a experimental apparatus, specifically, the single-link flexible manipulator shown in Fig. 2. This test-bed is manufactured by Quanser Consulting Inc. [27], and is in fact a two-link apparatus. We have removed the second link thus creating a single-link test bed. The motor and gearbox usually used to move the second link remain affixed to the end of the first link thus acting as a large payload. When we say large, we are referring to the fact the payload is much more massive than the slender flexible link.

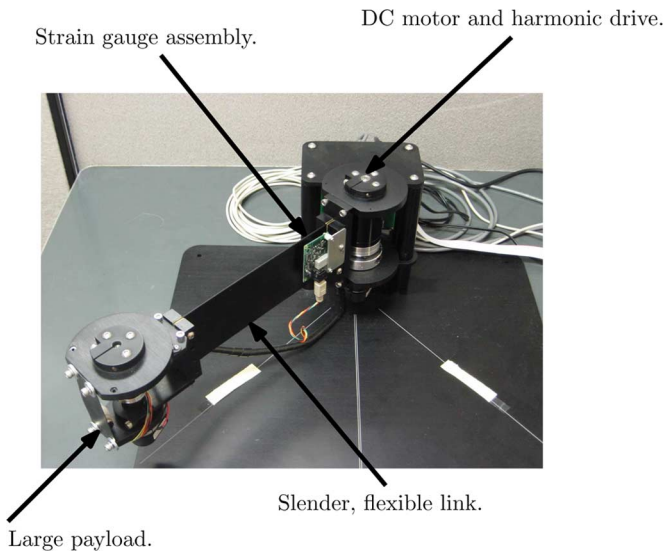

Fig. 2. Single-link flexible robot experiment manufactured by Quanser Consulting Inc.

The flexible link is made of steel, is 210.00 mm long, 1.27 mm thick, and 76.20 mm high. The payload mass is 0.6 kg, while the hub inertia (including the gearbox) is 6.4×10^{-2} kg·m^2. The flexible links first natural frequency is 19.5 rad/s. Affixed to the base of the link is a strain gauge, while a digital encoder is mounted to the output shaft of the motor. The encoder provides a measurement of θ, and the strain gauge and encoder together can be used to calculate the true tip position, ρ. Thus, as mentioned in Section II-B, ρ_μ can be calculated via (4) and proportional control can be implemented in a straightforward manner. In practice, the proportional control gain is set to $K_p = 20$ N/m. Note that $\dot{\theta}$ and $\dot{\rho}$ are not directly measured, and as mentioned in Section II-B, $\dot{\rho}_\mu$ will be acquired by filtering $\rho_\mu(s)$ using the derivative filter $f(s)$ shown in (6), where $\omega_f = 45$ rad/s and $\zeta_f = 1.15$. Readers interested in other specific details of the apparatus are referred to [27].

Guided by the theoretical developments of [14] μ was found to be approximately 0.4. However, [14] only provides an estimate of μ; in practice $\mu = 0.6$ is used which satisfies $0 \leq \mu < 1$ and, after experimental testing, was found to provide better closed-loop performance.

B. Passivity Violation Approximation

In order to design and implement a hybrid controller we must estimate various parameters associated with the hybrid passivity/finite gain stability theorem such as the critical frequency ω_c and γ_1. Recall from Section IV that $\delta_1 = 0$ and $\kappa_1 \approx \infty$. It is reasonable to assume $\delta_1 = 0$ because the ideal plant is passive, but also because at the point passivity is violated $\delta_1 = 0$ by definition. With respect to κ_1, the flexible system will have some natural damping (both rigid body and modal damping), therefore κ_1 is realistically large, but not infinite. We assume so mainly because it is difficult to estimate the damping of the system, and hence estimate κ_1.

To estimate ω_c and γ_1 we will consider our ideal plant and the affect of $f(s)$, as discussed in Section II-B. Recall from Section II-B that $g_p(s) = \rho_\mu(s)/u(s)$ is the

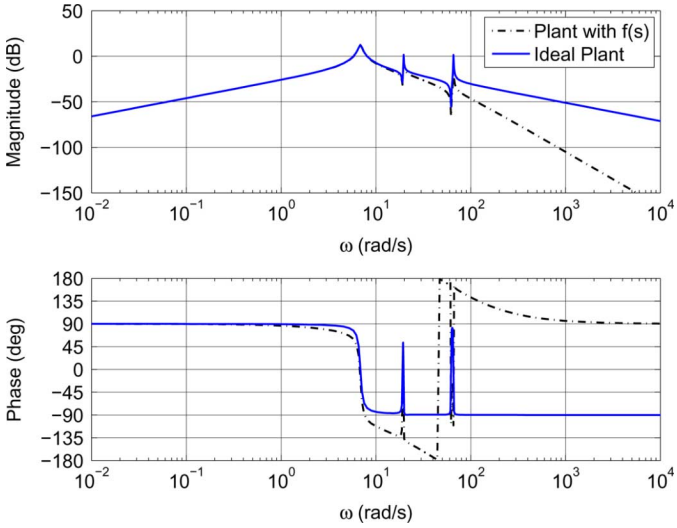

Fig. 3. Frequency response of ideal and perturbed plant. The ideal plant includes a pure derivative operator s, while the perturbed plant includes the derivative filter $f(s)$.

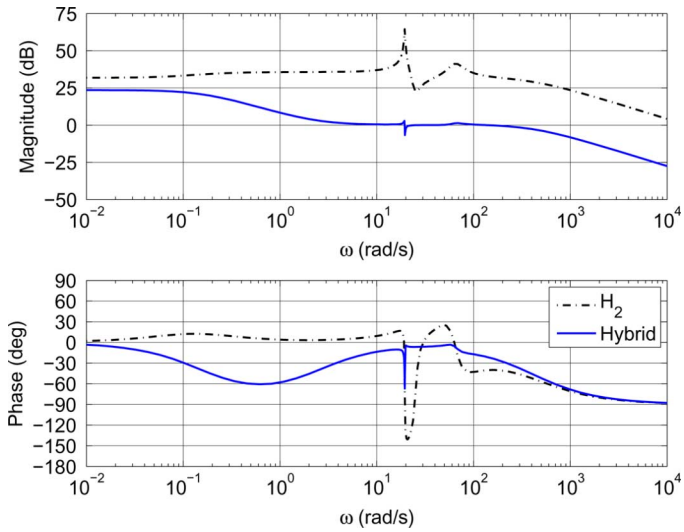

Fig. 4. Frequency response of $\mathcal{H}_2$ controller and hybrid passive/finite gain controller.

plant compensated with proportional control. As such, $g_1^\star(s) = sg_p(s) = \dot{\rho}_\mu(s)/u(s)$ represents the ideal passive/positive real plant, while $g_1(s) = f(s)g_p(s) = y_1(s)/u(s)$ is the perturbed plant that uses the derivative filter $f(s)$ to estimate $\dot{\rho}_\mu$. Both $g_1^\star(s)$ and $g_1(s)$ are shown in Fig. 3; clearly the ideal plant $g_1^\star(s)$ is positive real (i.e., has phase bounded by $\pm 90°$). The system $g_1(s)$ is positive real up until approximately 8.25 rad/s. Above this frequency $g_1(s)$ has finite gain, but does not behave passively. The system $g_1(s)$ is clearly hybrid possessing a passive region below 8.25 rad/s, and a non-passive but finite gain region above 8.25 rad/s.

Given the assumed frequency response of $g_1(s)$ in Fig. 3, ω_c and γ_1 of $g_1(s)$ are chosen to be 8.25 rad/s and 0.85 $\mathrm{m}/(\mathrm{N}\cdot\mathrm{s})$. It should be stressed that we can only estimate ω_c and γ_1; given our original plant model and an idea of how the sensors behave, we are estimating the value of ω_c. In turn, we are estimating the range where the plant behaves passively, and above such range we are confident the plant has finite gain, but again, we are estimating the gain γ_1 as well.

C. Controller Optimization Results

The numerical optimization formulation of Section IV will be used to design a hybrid controller for the single-link manipulator under consideration. The nominal plant used as the basis for optimization is $g_1^\star(s)$ (i.e., the "perfect" plant augmented with proportional control). The weights $\mathbf{D}_{12}^{\mathsf{T}}\mathbf{D}_{12} = 1 \times 10^{-2}$ and $\mathbf{D}_{21}\mathbf{D}_{21}^{\mathsf{T}} = 1 \times 10^{-4}$ are used for controller synthesis. Recall the use of the transfer function $\mathbf{W}(s)$ within the general MIMO optimization formulation; in the SISO context this filter is just the transfer function $w(s)$, which we will specify to be a fourth order lowpass Butterworth transfer function with a bandwidth of $\omega_o = 100$ rad/s. By choosing this bandwidth the optimization algorithm neglects differences in the magnitude responses of the $\mathcal{H}_2$ controller and the hybrid controller being optimized above ω_o. We do this because we expect the hybrid controller to roll-off owing to the high frequency gain constraint $\gamma_1\gamma_2 < 1$. At the same time, we desire our hybrid controller to perform well at low frequency, and should mimic the $\mathcal{H}_2$ controller as closely as possible.

During optimization, δ_2, κ_2, and γ_2 can be calculated in order to enforce the required optimization constraints. Specifically, for a SISO controller $g_2(s)$ $\delta_2 = \inf_{-\omega_c<\omega<\omega_c}\mathrm{Re}\{g_2(j\omega)\}$, $\kappa_2 = \sup_{-\omega_c<\omega<\omega_c}|g_2(j\omega)|$, and $\gamma_2 = \sup_{\omega\geq\omega_c}|g_2(j\omega)|$ as presented in Section III-B.

The frequency response of the numerically optimized hybrid controller, $g_2(s)$, as well as the traditional $\mathcal{H}_2$ controller, $g_2^\star(s)$, used within the optimization formulation are shown in Fig. 4. The gain of the $g_2(s)$ is less than the gain of $g_2^\star(s)$ over all frequencies. Because $\gamma_1\gamma_2 < 1$ must be satisfied above ω_c, the gain of $g_2(s)$ is reduced over all frequencies (including DC). Notice that at approximately 19.6 and 66.0 rad/s the magnitude of the $\mathcal{H}_2$ controller increases. The hybrid controller also has a slight increase in gain at these two frequencies. Similarly, at 19.6 rad/s the phase of $g_2^\star(s)$ dips below $-135°$, and $g_2(s)$ attempts to mimic the phase response by dipping to $-65°$. Clearly the hybrid controller is attempting to mimic the $\mathcal{H}_2$ controller as best it can while satisfying a low frequency phase constraint and high frequency gain constraint.

Referring to Fig. 3, notice the flexible links lower two modes are excited at approximately 19.6 and 66.0 rad/s. The gain increase in both $g_2(s)$ and $g_2^\star(s)$ at 19.6 and 66.0 rad/s can be attributed to damping these two modes.

Consider the open-loop frequency response of $g_1^\star(s)$ and $g_2^\star(s)$, as well as $g_1^\star(s)$ and $g_2(s)$ shown in Fig. 5. Notice that the overall shape of the two frequency responses is similar. Because the hybrid controller $g_2(s)$ was designed to mimic the $\mathcal{H}_2$ controller $g_2^\star(s)$, it is logical that the open-loop frequency response $g_1^\star(s)g_2(s)$ mimics the open-loop frequency response of $g_1^\star(s)g_2^\star(s)$. When controlled by the $\mathcal{H}_2$ controller $g_2^\star(j\omega)$, the ideal system can tolerate a gain decrease of 5.1 dB (at 25.0 rad/s) before instability, while the phase margin is 49.6° (at 131 rad/s). When the hybrid controller $g_2(j\omega)$ is used to control $g_1^\star(j\omega)$, the system is significantly more robust; the gain margin

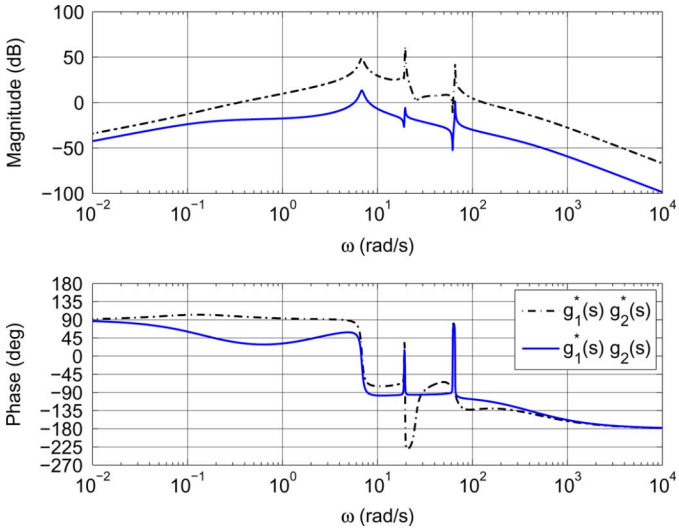

Fig. 5. Frequency response of open-loop systems $g_1^\star(j\omega)g_2^\star(j\omega)$ and $g_1^\star(j\omega)g_2(j\omega)$.

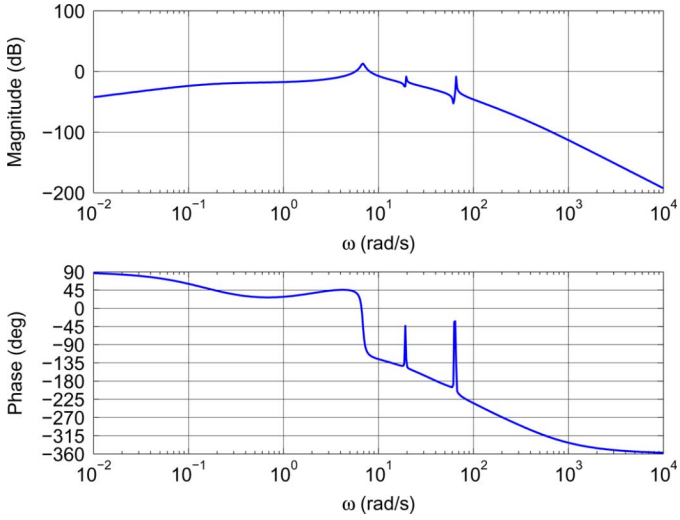

Fig. 6. Frequency response of open-loop system $g_1(j\omega)g_2(j\omega)$.

is infinite, while the phase margin is 86.9° (at 8.16 rad/s). The gain margin is infinite because, by chance (that is to say, not by design on our part), the optimal hybrid controller is actually SPR over all frequencies, not just at low frequency. It is well known the gain margin associated with a positive real plant being controlled by a SPR controller is infinite.

Now let's investigate how the robustness properties of the system change (in terms of gain margin and phase margin) when $g_2^\star(s)$ and $g_2(s)$ are used to control $g_1(s)$, the plant that uses $f(s)$ to acquire rate information. Interestingly, when the $\mathcal{H}_2$ controller $g_2^\star(s)$ is used to control $g_1(s)$, the closed-loop is unstable. As such, plotting the open-loop frequency response $g_1(j\omega)g_2^\star(j\omega)$ is meaningless, as is stating gain and phase margins. When $g_2(s)$ is used to control $g_1(s)$ the closed-loop system is stable (as we would expect), but the gain and phase margins are quite good as well. The open-loop frequency response $g_1(s)g_2(s)$ is shown in Fig. 6. The gain margin is 14.3 dB ($\phi_{gm} = 66.0$ rad/s) while the phase margin is 64.3° ($\phi_{pm} = 8.1$ rad/s). These margins indicate the closed-loop system is quite robust in that the system can tolerate additional perturbations before instability ensues. Compared to the perfect plant being controlled by $g_2(s)$, although the gain and phase margins are deteriorated when $f(s)$ is present, they have not been destroyed all together.

D. Experimental Results

The controllers $g_2(s)$ and $g_2^\star(s)$ depicted in Fig. 4 have been used to control the single-link flexible manipulator apparatus depicted in Fig. 2. The manipulator is to follow a desired trajectory, $\rho_d = J_\theta\theta_d$, starting at $\rho_a = J_\theta\theta_a$, moving to $\rho_b = J_\theta\theta_b$, then moving back to ρ_a. Specifically, $\theta_a = -\pi/4$ rad, while $\theta_b = \pi/4$ rad. The desired trajectory between set points is

$$\theta_d = \left[10\left(\frac{t}{t_f}\right)^3 - 15\left(\frac{t}{t_f}\right)^4 + 6\left(\frac{t}{t_f}\right)^5\right](\theta_f - \theta_i) + \theta_i$$

where t_f is 2 s, θ_f is the final angular position, and θ_i is the initial angular position. Between maneuvers there is a 2 s dwell.

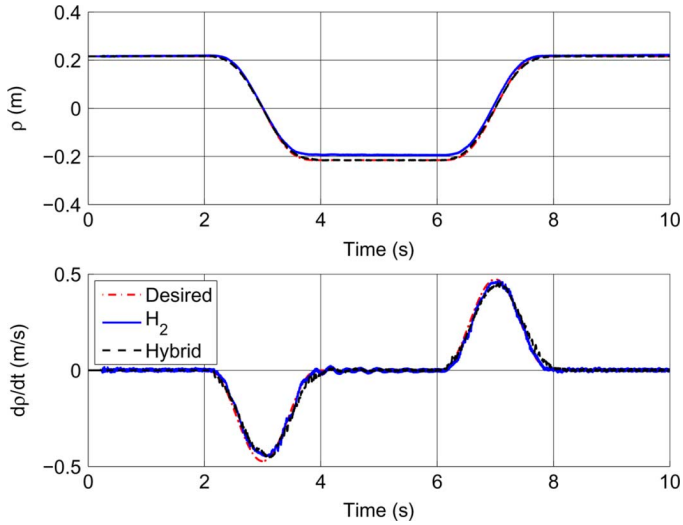

Fig. 7. System response: tip position and tip rate.

Fig. 7 shows the system response of the manipulator as controlled by the hybrid controller and $\mathcal{H}_2$ controller, while Fig. 8 shows the system response error where $e = \rho - \rho_d$. The rms error is shown in Table I; the hybrid control outperforms the traditional $\mathcal{H}_2$ controller. In Fig. 7 one can see, especially around 4 s, that the $\mathcal{H}_2$ controller does not suppress the tip-rate as quickly as the hybrid controller does. The hybrid controller is a better rate controller. With respect to tip position errors, the system controlled by $g_2^\star(s)$ never reaches a steady-state tip position error of zero, as shown in the tip position plot of Fig. 7 and the tip position error plot of Fig. 8. This can be attributed to the fact that the gearbox stiction (i.e., static friction) is not perfectly compensated, and there is no integral term (with respect to the μ-tip position) in the feedback control loop that would force zero steady-state tip position error. The system controlled by $g_2(s)$ has basically zero steady-state tip position error because both the rate and position tracking are quite good as the manipulator slews to and from each set-point, and hence the error upon completion of the maneuver is very small.

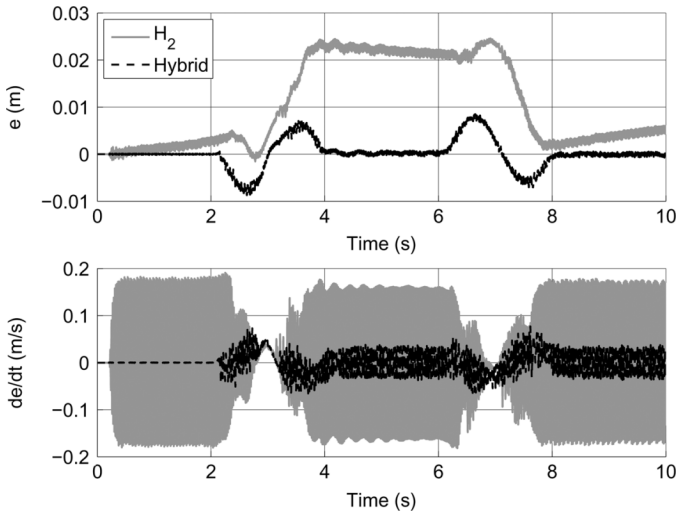

Fig. 8. System response error: tip position error and tip rate error.

TABLE I
SYSTEM RESPONSE RMS ERROR

	e_{rms} (m)	$\dot{e}_{rms}$ (m/s)
Hybrid Control	2.664×10^{-3}	2.258×10^{-2}
$\mathcal{H}_2$ Control	13.058×10^{-3}	10.7074×10^{-2}

The hybrid controller performs well for a variety of reasons. Recall that the hybrid controller is optimally designed assuming an accurate plant model within a low frequency range (i.e., $\omega \in (-\omega_c, \omega_c)$). Therefore, the hybrid controller approximates the optimal $\mathcal{H}_2$ controller as best it can at low frequency while satisfying the hybrid passivity/finite gain stability requirements. Particularly, the hybrid controller has higher gain at low frequency, gain increases at certain frequencies (i.e., 19.6 and 66.0 rad/s), and a phase response that tries to approximates the $\mathcal{H}_2$ solution. However, above ω_c, where passivity has been violated and it is assumed the nominal plant model is not representative of the true system, the controller rolls-off, essentially ignoring high frequency information contained in the feedback measurement. Additionally, the high frequency gain constraint forces the controller to have gain that is less than the $\mathcal{H}_2$ controller in the passive band. This rejection of high frequency data, and noise, but retention of "good" low frequency data yields the performance observed.

On the other hand, the $\mathcal{H}_2$ controller assumes the nominal plant is accurate over all frequencies, including the region where passivity has been violated. The gain of the $\mathcal{H}_2$ controller is (relatively) high above ω_c, where the nominal plant model does not accurately represent the true plant. Additionally, the gain profile of the $\mathcal{H}_2$ controller does not reject high frequency noise, which is amplified, as shown in the error signals of Fig. 8.

It is interesting to see that although that closed-loop involving $g_1(s)$ (the plant with $f(s)$) and $g_2^\star(s)$ is theoretically unstable, the $\mathcal{H}_2$ controller stabilizes the physical manipulator test-bed. This fact highlights the reality that our plant and derivative filter model representing $g_1(s)$ do not capture the true dynamics of the system.

E. Attempted Modifications to the Controller Optimization Scheme

It is unfortunate that the optimal hybrid controller $g_2(s)$ has gain that is less than that of $g_2^\star(s)$ at low frequency (see Fig. 4). It would be ideal if the low frequency gain of $g_2(s)$ was closer to that of $g_2^\star(s)$, thus realizing better performance. An attempt was made to do so; within the optimization formulation another constraint was added in which the DC gain of $g_2(s)$ had to be greater than or equal to the DC gain of $g_2^\star(s)$, i.e., $|g_2(j0)| \geq |g_2^\star(j0)|$. It was found that this constraint severely conflicted with the constraint $\gamma_1\gamma_2 < 1$, and as such the optimization procedure could not converge (i.e., no solution was found). The constraint $|g_2(j0)| \geq |g_2^\star(j0)|$ pushes the low frequency gain of $g_2(s)$ up, while the constraint $\gamma_1\gamma_2 < 1$ pulls down the gain of $g_2(s)$ around and above ω_c. The controller cannot satisfy $|g_2(j0)| \geq |g_2^\star(j0)|$, roll-off fast enough to satisfy $\gamma_1\gamma_2 < 1$, *and* satisfy the required low frequency phase constraint $\delta_2 > 0$. However, if ω_c were much larger (e.g., 100 or 1000 rad/s), then including $|g_2(j0)| \geq |g_2^\star(j0)|$ may be tolerable because $g_2(s)$ would not have to roll-off as fast in the low frequency passive/positive real frequency band.

Picking different ω_o values during the optimization process was also investigated. Recall that ω_o is the frequency where $w(s)$ rolls off. For example, when ω_o is set to 30 rad/s, the optimization scheme converges, however, it was found the resultant controller did not perform as well $g_2(s)$, the controller shown in Fig. 4 which was optimized using $\omega_o = 100$ rad/s. The reason is related to having the controller suppress the second vibration mode of the link. The $\mathcal{H}_2$ controller gain is high at 66.0 rad/s, and hence $g_2^\star(s)$ suppresses the second vibration mode of the link. When the cutoff of $w(s)$ is set to 100 rad/s, the hybrid controller is forced to mimic the $\mathcal{H}_2$ controller (or, said another way, penalized if it does not mimic $\mathcal{H}_2$ controller), and hence the hybrid controller tries to suppress the vibration mode at 66.0 rad/s just as the $\mathcal{H}_2$ controller does. However, when the cutoff of $w(s)$ is set to 30 rad/s the hybrid controller synthesized during optimization is not penalized for not mimicking the the $\mathcal{H}_2$ controller above 30 rad/s; the resultant hybrid controller essentially ignores the vibration mode at 66.0 rad/s that should be suppressed, which was found to lead to a decrease in closed-loop performance.

VI. CLOSING REMARKS

In this paper we considered the design and optimization of a hybrid passivity/finite gain controller to control a single-link flexible manipulator which has experienced a passivity violation. After discussing the single-link flexible manipulator model and the relevant passive input-output mapping, hybrid systems theory was reviewed in a LTI, SISO context. We discussed δ, ϵ, and γ in terms of phase and gain in different frequency bands. The hybrid passivity/finite gain stability theorem was also stated, and briefly discussed in terms of its relation to the traditional passivity and small gain theorems. Next, a numerical optimization problem was posed whereby a hybrid controller was designed to mimic a traditional $\mathcal{H}_2$ controller subject to constraints dictated by the hybrid passivity/finite gain stability theorem. Experimental results confirmed the success of the

optimal hybrid controller found relative to a traditional $\mathcal{H}_2$ controller.

In this paper we have focused on the control of a single-link system to fully elucidate the hybrid theory and μ-tip rate control in a SISO context. However, we would like to reiterate that the hybrid theory presented is also applicable to nonlinear MIMO systems, as discussed in [18]. Future work will consider joint-based control of a two-link manipulator where joint rates are acquired via a derivative filter. For n-link flexible robotic systems, it is well known that the map between joint torques and joint rates is passive. However, as in this paper, acquiring rate information via a derivative filter induces a passivity violation. Similarly, the μ-tip theory used in this paper to control the tip-rate of the single-link manipulator is equally applicable to n-link manipulators provided the manipulator is carrying a large payload; this is demonstrated in [13]. Unfortunately, our two-link experimental apparatus is not designed to carry a massive payload, thus μ-tip theory can not be used, which is why our future work will focus on joint-based control of a two-link manipulator.

In addition to more experimental work (i.e., two-link manipulator control), another research area we intend on perusing is the control of systems that can be described in terms of three regions: a passive region, an intermediate passive and finite gain region, and a finite gain region where passivity has been violated. Such an extension would be similar, although not identical, to the mixed systems frame work presented in [19] and [20]. Additionally, less conservative means to synthesize hybrid controllers will be investigated in the future. It is hoped that we can pose a convex optimization problem where the hybrid controller constraints are enforced using linear matrix inequalities.

ACKNOWLEDGMENT

The authors would like to thank the anonymous reviewers and the associate editor for their excellent comments. The changes made as a result of the thorough and insightful reviews have improved the paper greatly.

REFERENCES

[1] B. D. O. Anderson and S. Vongpanitlerd, *Network Analysis and Synthesis*. Englewood Cliffs, NJ: Prentice-Hall, 1973.

[2] R. Ortega, A. Loria, P. J. Nicklasson, and H. Sira-Ramirez, *Passivity-Based Control of Euler-Lagrange Systems*. London, U.K.: Springer, 1998.

[3] C. A. Desoer and M. Vidyasagar, *Feedback Systems: Input-Output Properties*. New York: Academic Press, 1975.

[4] M. J. Balas, "Active control of flexible systems," *J. Opt. Theory Appl.*, vol. 25, pp. 415–436, Jul. 1978.

[5] M. J. Balas, "Feedback control of flexible systems," *IEEE Trans. Autom. Control*, vol. 23, pp. 673–679, Aug. 1978.

[6] J. L. Junkins and Y. Kim, *Introduction to Dynamics and Control of Flexible Structures*. Washington, DC: American Inst. Aeronautics and Astronautics, Inc., 1993.

[7] C. J. Damaren, "Modal properties and control system design for two-link flexible manipulators," *Int. J. Robot. Res.*, vol. 17, pp. 667–678, Jun. 1998.

[8] R. J. Benhabib, R. P. Iwens, and R. L. Jackson, "Stability of large space structure control systems using positivity concepts," *J. Dyn. Syst., Meas., Control*, vol. 4, pp. 487–494, Sep.–Oct. 1981.

[9] M. D. McLaren and G. L. Slater, "Robust multivariable control of large space structures using positivity," *J. Dyn. Syst., Meas., Control*, vol. 10, pp. 393–400, Jul.–Aug. 1987.

[10] J. R. Forbes and C. J. Damaren, "Design of gain-scheduled strictly positive real controllers using numerical optimization for flexible robotic systems," *J. Dyn. Syst., Meas., Control*, vol. 132, no. 3, pp. 034503-1–034503-7, 2010.

[11] W. B. Gevarter, "Basic relations for control of flexible vehicles," *AIAA J.*, vol. 8, no. 4, pp. 666–671, 1970.

[12] C. J. Damaren, "Passivity analysis for flexible multilink space manipulators," *J. Guid., Control, Dyn.*, vol. 18, pp. 272–279, Mar.–Apr. 1995.

[13] E. G. Christoforou and C. J. Damaren, "The control of flexible-link robots manipulating large payloads: Theory and experiments," *J. Robot. Syst.*, vol. 17, pp. 255–271, May–Jun. 2000.

[14] C. J. Damaren, "Passivity and noncollocation in the control of flexible multibody systems," *J. Dyn. Syst., Meas., Control*, vol. 122, no. 1, pp. 11–17, 2000.

[15] D. Wang and M. Vidyasagar, "Passive control of a single flexible link," in *Proc. IEEE Int. Conf. Robot. Autom.*, 1990, pp. 1432–1437.

[16] H. Pota and M. Vidyasagar, "Passivity of flexible beam transfer functions with modified outputs," in *Proc. IEEE Int. Conf. Robot. Autom.*, 1991, pp. 2826–2831.

[17] A. D. Luca, P. Lucibello, and G. Ulivi, "Inversion techniques for trajectory control of flexible robot arms," *J. Robot. Syst.*, vol. 6, no. 4, pp. 325–344, 1989.

[18] J. R. Forbes and C. J. Damaren, "A hybrid passivity and finite gain stability theorem: Stability and control of systems possessing passivity violations," *IET Control Theory Appl.*, vol. 4, no. 9, pp. 1795–1806, 2010.

[19] W. M. Griggs, B. D. Anderson, and A. Lanzon, "A "mixed" small gain and passivity theorem in the frequency domain," *Syst. Control Lett.*, vol. 56, pp. 596–602, Sep.–Oct. 2007.

[20] W. M. Griggs, B. D. Anderson, A. Lanzon, and M. C. Rotkowitz, "Interconnections of nonlinear systems with "mixed" small gain and passivity properties and associated input-output stability results," *Syst. Control Lett.*, vol. 58, pp. 289–295, Apr. 2009.

[21] T. Iwasaki, S. Hara, and H. Yamauchi, "Dynamical systems design from a control perspective: Finite frequency positive-realness approach," *IEEE Trans. Autom. Control*, vol. 48, no. 8, pp. 1337–1354, Aug. 2003.

[22] R. H. Cannon, Jr. and E. Schmitz, "Initial experiments on the end-point control of a flexible one-link robot," *Int. J. Robot. Res.*, vol. 3, pp. 62–75, Sep. 1984.

[23] M. Vidyasagar, *Nonlinear Systems Analysis*, 2nd ed. Englewood Cliffs, NJ: Prentice-Hall, 1993.

[24] M. Green and D. J. N. Limebeer, *Linear Robust Control*. Upper Saddle River, NJ: Prentice-Hall, 1995.

[25] C. J. Damaren, H. J. Marquez, and A. G. Buckley, "Optimal strictly positive real approximations for stable transfer functions," *IEE Proc. —Control Theory Appl.*, vol. 143, pp. 537–542, Nov. 1996.

[26] J. Nocedal and S. J. Wright, *Numerical Optimization*, 2nd ed. London, U.K.: Springer, 2000.

[27] Quanser Consulting Inc., Markham, ON, Canada, "2-DOF serial flexible link robot reference manual," Doc. No. 763, Rev. 1, 2008.

James Richard Forbes was born in Kitchener, ON, Canada, in 1982. He received the B.A.Sc. degree in mechanical engineering (Honours, Co-op) from the University of Waterloo, Waterloo, ON, Canada, in 2006, and the M.A.Sc. degree in aerospace science and engineering from the University of Toronto Institute for Aerospace Studies, Toronto, ON, Canada, in 2008, where he is currently pursuing the Ph.D. in aerospace science and engineering.

The focus of his current research is linear and nonlinear control of aerospace systems including large flexible space structures and spacecraft.

Christopher Damaren was born in Toronto, ON, Canada, in 1962. He received the B.A.Sc. degree in engineering science (aerospace option) from the University of Toronto, Toronto, ON, Canada, in 1985, and the M.A.Sc. and Ph.D. degrees from the University of Toronto Institute for Aerospace Studies (UTIAS), Toronto, ON, Canada, in 1987 and 1990, respectively, both in aerospace engineering.

From 1990 to 1995, he was an Assistant Professor with the Department of Engineering, Royal Roads Military College, Victoria, BC, Canada. From 1995 to 1999, he was a Senior Lecturer with the Department of Mechanical Engineering, University of Canterbury, Christchurch, New Zealand. Since 1999, he has been with UTIAS, where he is currently a Professor. His research interests include the areas of dynamics and control of space systems.

Prof. Damaren is a Fellow of the Canadian Aeronautics and Space Institute and an Associate Fellow of the American Institute of Aeronautics and Astronautics.